

Microstructure development and precipitation effects in ultra fine grained Mg-3Tb-2Nd alloy prepared by high pressure torsion*

Jakub Cizek^{1, a}, Ivan Prochazka¹, Bohumil Smola¹, Ivana Stulikova¹, Martin Vlach¹, Rinat K. Islamgaliev² and Olya Kulyasova²

¹Faculty of Mathematics and Physics, Charles University, Prague, Czech Republic

²Institute of Physics of Advanced Materials, Ufa State Aviation Technical University,
Ufa 450000, Russia.

^ajakub.cizek@mff.cuni.cz

Keywords: Mg-alloys, positron annihilation, precipitation, high pressure torsion.

Abstract. Mg-Tb-Nd ternary alloy represents a novel hardenable Mg-based alloy with enhanced strength and favorable creep properties. In the present work we studied microstructure of ultra fine grained (UFG) Mg-Tb-Nd alloy prepared by high pressure torsion (HPT). Lattice defects introduced into the specimen by the severe plastic deformation play a key role in physical properties of UFG specimens. It is known that positron lifetime (PL) spectroscopy is highly sensitive to open volume defects (like vacancies, dislocations, etc.). Therefore, PL spectroscopy is an ideal tool for defect characterizations in the HPT deformed specimens. In the present work we combined PL studies with transmission electron microscopy and microhardness measurements. After detailed characterization of the as-deformed structure, the specimens were step-by-step isochronally annealed and we investigated the development of microstructure with increasing temperature.

Introduction

Low density Mg-based alloys allow for a significant weight reduction which raises the effectiveness in a broad range of industrial applications. Unfortunately, use of most of Mg alloys is limited to low temperatures due to a degradation of their mechanical properties above 200°C. There are several approaches how to overcome this problem. Particularly promising way is use of non-traditional rare earth alloying elements [1]. Mg-Tb-Nd ternary alloy is a novel hardenable alloy with enhanced strength and favorable creep properties even at elevated temperatures [2]. Despite the favorable strength and thermal stability, a disadvantage of this alloy consists in a poor ductility insufficient for most of potential industrial applications. Grain refinement is a well-known method how to improve ductility of metallic materials. Hence, severe plastic deformation (SPD), which is able to fabricate UFG structure, could represent a promising way for improvement of properties of Mg-alloys due to the effects of an extreme grain size reduction. The aim of this work is microstructure characterization of Mg-Tb-Nd alloy prepared by HPT [3] and its comparison with microstructure of corresponding coarse-grained material. Subsequently, decomposition of supersaturated solid solution (sss) and precipitation effect in UFG and coarse-grained alloy were compared. Defects introduced by SPD play key role in the UFG structure. Detailed characterization of these defects represents, therefore, an important task in microstructure investigations of the UFG materials. For this reason we employed positron lifetime (PL) spectroscopy, which represents a well established non-destructive technique with a high sensitivity to open-volume defects like vacancies, dislocations, etc. [4]. Thus, PL spectroscopy is an ideal tool for defects studies of UFG materials. In this work we combined PL studies with transmission electron microscopy and Vickers microhardness (HV) investigations.

*This work was supported by the Ministry of Education of Czech Republic (project MS 0021620834), The Academy of Science of Czech Republic (projects KAN300100801) and The Czech Science Foundation (project 106/06/0252).

Experimental

Specimens of pure Mg (99.95%) and Mg-3wt.%Tb-2wt.%Nd (Mg₃Tb₂Nd) alloy prepared by squeeze casting were investigated. Results of chemical analysis of the alloy and the original Mg material are given in Table 1. The as-cast alloy was subjected to a solution annealing at 525°C for 6 hours. This treatment is sufficient to dissolve the alloying elements completely [5]. The solution annealing was finished by quenching into water of room temperature. To fabricate the UFG structure, the as-received Mg and the solution treated Mg₃Tb₂Nd alloy were deformed by HPT at room temperature using 5 rotations under a high pressure of 6 GPa. After detailed characterization of the as deformed microstructure, the specimens were subjected to step-by-step isochronal annealing (20°C/20 min). Each annealing step was finished by quenching into water of room temperature and subsequent investigations performed at room temperature.

Material	Gd	Tb	Nd	Mn	Fe	Zn	Al	Si	Cu	Ni	Mg
Mg	-	-	-	0.014	0.020	0.0001	0.0077	0.0090	0.0026	0.0004	balance
Mg ₃ Tb ₂ Nd	-	3.15	1.75	0.014	0.020	0.0001	0.0077	0.0090	0.0026	0.0004	balance

Table 1 Chemical composition (in weight %) of the studied materials.

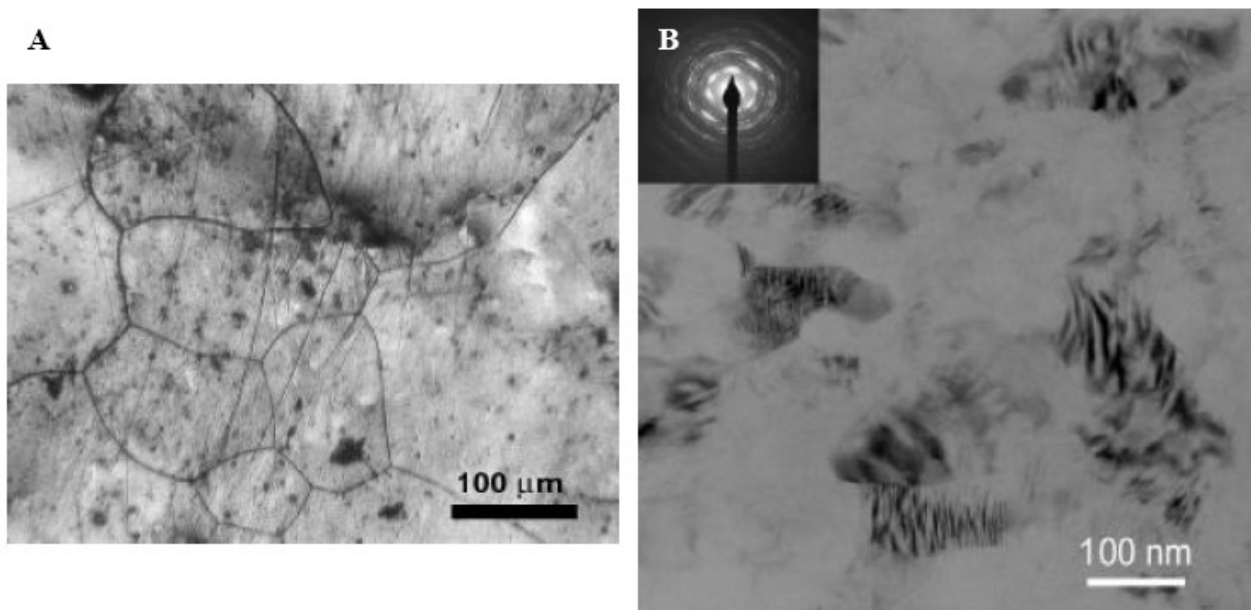


Fig. 1 Micrographs of MgTb₃Nd₂ alloy: (A) solution treated coarse-grained specimen – optical microscopy, (B) specimen with UFG structure prepared by HPT (as-deformed state) - TEM.

Sample	τ_1 (ps)	I_1 (%)	τ_2 (ps)	I_2 (%)	ρ_D (10^{13} m^{-2})
Mg, well annealed	225.3 ± 0.4	100	-	-	< 0.1
Mg, HPT deformed	188 ± 5	39 ± 1	257 ± 3	61 ± 1	0.9 ± 0.1
Mg ₄ Tb ₂ Nd, solution treated	220 ± 1	91 ± 1	280 ± 20	9 ± 1	< 0.1
Mg ₄ Tb ₂ Nd, HPT deformed	100 ± 10	6.2 ± 0.8	256 ± 2	93.8 ± 0.5	8.0 ± 0.9

Table 2 A summary of PL spectroscopy results for the studied specimens.

A fast-fast PL spectrometer similar to that described in [6] with time resolution of 160 ps was used in this work. The TEM observations were carried out on a JEOL 2000 FX electron microscope operating at 200 kV. The Vickers microhardness, HV, was measured at load of 100 g applied for 10 s using STRUERS Duramin 2 hardness tester.

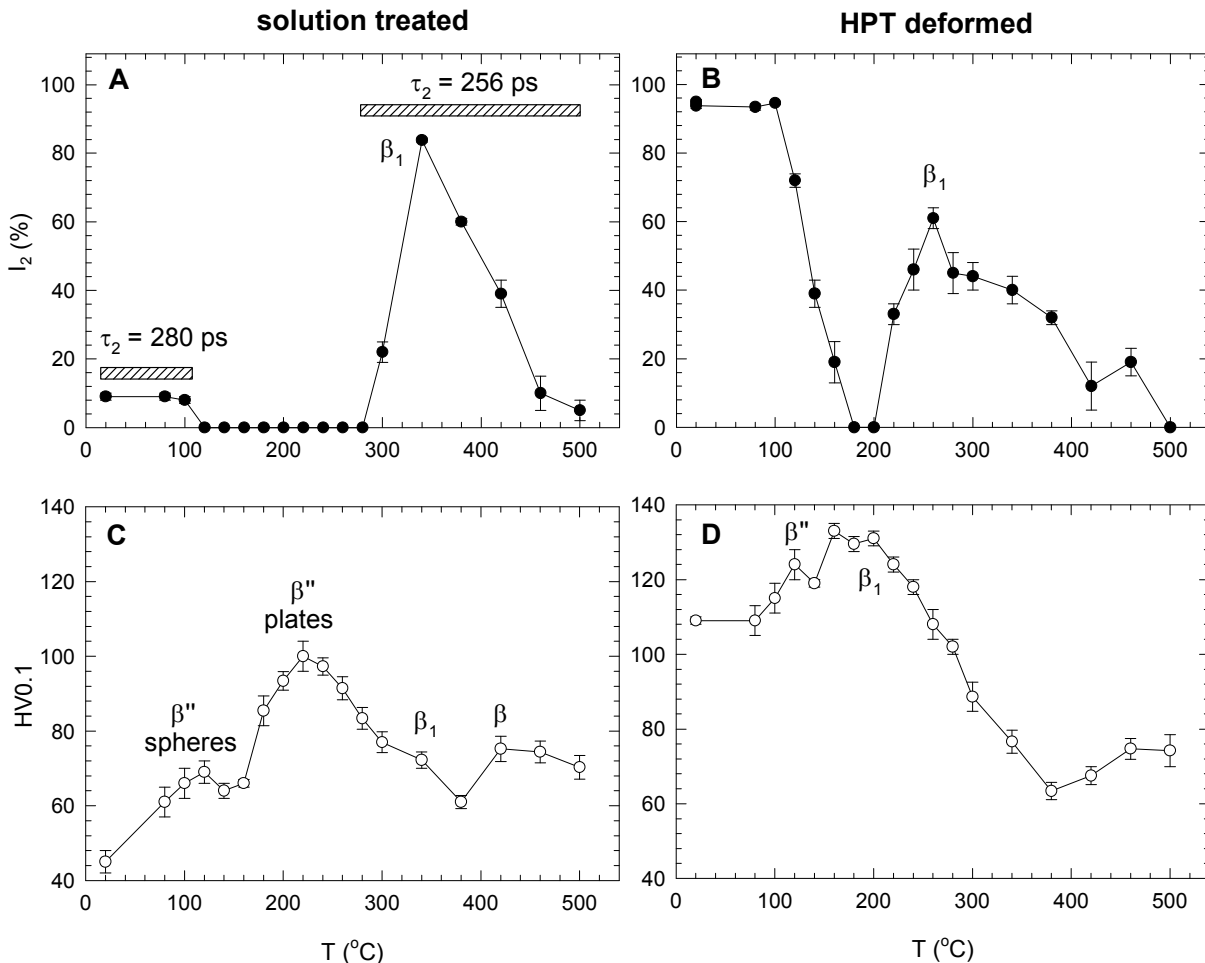


Fig. 2 Dependence of intensity I_2 of positrons trapped at defects on annealing temperature: (A) solution-treated alloy, (B) UFG alloy. Dependence of microhardness on annealing temperature: (C) solution-treated alloy, (D) UFG alloy.

Results and Discussion

Pure Mg. Positron lifetimes τ_i and the relative intensities I_i of the components resolved in the PL spectra of the studied specimens are listed in Table 2. The well annealed Mg reference specimen exhibits a single component PL spectrum with lifetime $\tau_B = 225$ ps which agrees well with the calculated Mg bulk lifetime [7]. Thus, defect density in the reference Mg specimen is negligible and virtually all positrons annihilate from the free state. PL spectrum of the Mg specimen deformed by HPT can be well fitted by two components, see Table 2. The shorter component with lifetime $\tau_1 < \tau_B$ comes from free positrons, while the longer component with lifetime τ_2 is a contribution of positrons trapped at defects introduced by HPT. Lifetime of this component $\tau_2 \approx 256$ ps corresponds well with that of positrons trapped at dislocations in Mg [7]. Thus we can attribute this component to positrons trapped at dislocations introduced by HPT. Microstructure of HPT deformed Mg was investigated in our previous paper [8]. HPT deformed Mg exhibits a bimodal structure containing UFG regions with grain size 100-300 nm and a high dislocation density. However, UFG regions are separated by recrystallized regions with larger grains (5 μm) and low dislocation density. Hence, dynamical recovery of UFG microstructure takes place already during HPT processing in pure Mg. Dislocation density ρ_D in the specimen can be calculated using the two state trapping model [4]

$$\rho_D = \frac{1}{\nu_D} \frac{I_2}{I_1} \left(\frac{1}{\tau_B} - \frac{1}{\tau_2} \right), \quad (1)$$

where ν_D is the positron specific trapping rate to Mg-dislocation. In this paper we used the value $\nu_D = 1 \times 10^{-4} \text{ m}^2\text{s}^{-1}$ [4], which holds for majority of metals. The mean dislocation density ρ_D calculated from Eq. (1) is given in the last column in Table 2.

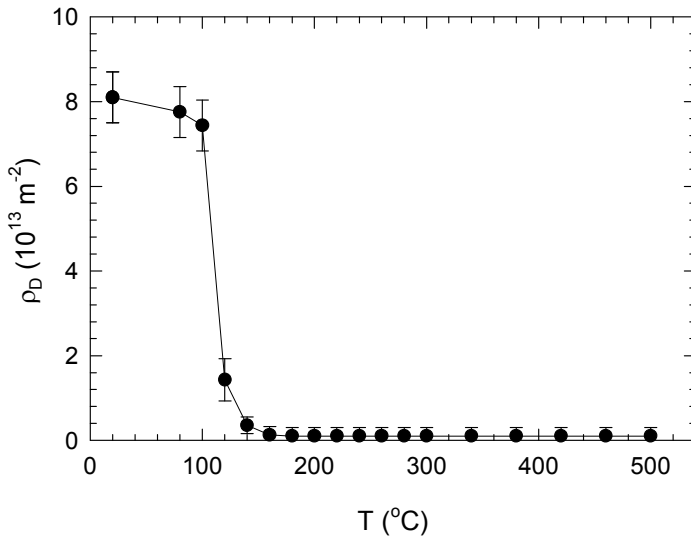


Fig. 3 Dependence of the mean dislocation density in HPT deformed Mg₃Tb₂Nd alloy on annealing temperature.

Coarse-Grained Mg₃Tb₂Nd Alloy. The solution-treated alloy exhibits a two component PL spectrum, see Table 2. The dominant contribution comes from free, delocalized positrons. However, a small fraction of positrons are trapped at quenched-in vacancies which remain “frozen” in the solution treated sample due to rapid cooling from the solution

temperature. Positrons trapped at quenched-in vacancies contribute to the component with lifetime ≈ 280 ps. Vacancies in Mg are not stable at room temperature, therefore, the observed defects are vacancies bound to Tb or Nd atoms. Similar type of defects, i.e. the quenched-in vacancies bound to Gd atoms, was found also in solution treated Mg-Gd alloy [7]. No contribution of positrons trapped at dislocations was found in the PL spectrum of the solution treated Mg₃Tb₂Nd. It testifies that dislocations were annealed out under detectable limit (below 10^{-12} m^{-2}). This conclusion is supported also by TEM observations. It should be also mentioned that no precipitates were observed by TEM in the solution treated alloy.

UFG Mg₃Tb₂Nd Alloy. A representative TEM image of HPT-deformed Mg₃Tb₂Nd alloy is shown in Fig. 1B. The specimen shows a homogeneous UFG structure with grain size ≈ 100 nm. The dominant component in PL spectrum has lifetime $\tau_2 \approx 256$ ps which comes from positrons trapped at dislocations. A high density of dislocations can be seen also in the TEM image. Dislocations are homogeneously distributed throughout whole grains. Electron diffraction pattern testifies long angle miss-orientation of neighboring grains. The specimen exhibits (00.1) type texture. No precipitates were found in the as-deformed alloy by TEM. A strong grain refinement and a high dislocation density lead to a substantial hardening reflected by an increase of microhardness: the HPT-deformed alloy exhibits about 140 % higher HV compared to the solution treated specimen.

Precipitation Effects. Fig. 2 shows Dependence of intensity I_2 of positrons trapped at defects and microhardness on annealing temperature. We start discussion of precipitation effects with the solution treated Mg₃Tb₂Nd alloy, which undergoes the following decomposition sequence: sss \rightarrow β'' (D019) \rightarrow β_1 (fcc) \rightarrow β (cubic, stable) [5]. The quenched-in vacancies are annealed out at 120°C which is seen in Fig. 2A as disappearance of the long lived component with lifetime $\tau_2 = 280$ ps. The sample exhibits a single component PL spectrum in the temperature range (120–280)°C, i.e. there are no active positron traps in this temperature interval. Precipitation of β'' phase particles starts around 80°C and causes a remarkable hardening, see Fig. 2C. The β'' phase particles are fully coherent with Mg lattice and, therefore, no open volume defects are introduced by β'' precipitation. Thus, PL spectroscopy is insensitive to the precipitation of β'' phase. TEM investigations revealed that fine spherical β'' phase precipitates transform into fine plates in the temperature interval (180–240)°C. One can see in Fig. 2C that it has a strong hardening effect with the peak hardness at 210°C.

Fine β'' phase plates precipitate in a triangular configuration parallel with the prismatic planes $\{11.0\}$. Further annealing up to 270°C leads to growth of the plate shaped precipitates (diameter 20-30 nm) reflected by a decrease of microhardness. At higher temperatures, β'' phase is transformed into β_1 phase with fcc structure. Plates (diameter 200-500 nm) of β_1 phase were observed by TEM in the alloy annealed up to 330°C . Formation of β_1 phase is accompanied by appearance of a defect component with lifetime $\tau_2 \approx 256$ ps in PL spectra. Intensity of this component steeply increases with annealing temperature up to a maximum at 340°C . Thus, new positron traps are introduced by β_1 phase precipitation. Positrons are most probably trapped at misfit defect at the precipitate-matrix interfaces. A decrease of I_2 above 340°C is due to dissolution of β_1 phase particles. This behavior is postponed in the temperature range $(390-450)^\circ\text{C}$ by formation of β phase (plate-shaped particles 2-3 μm in diameter). Precipitation of β phase causes a slight hardening seen in Fig. 2C. Above 450°C β phase precipitates dissolve and the solid solution is restored.

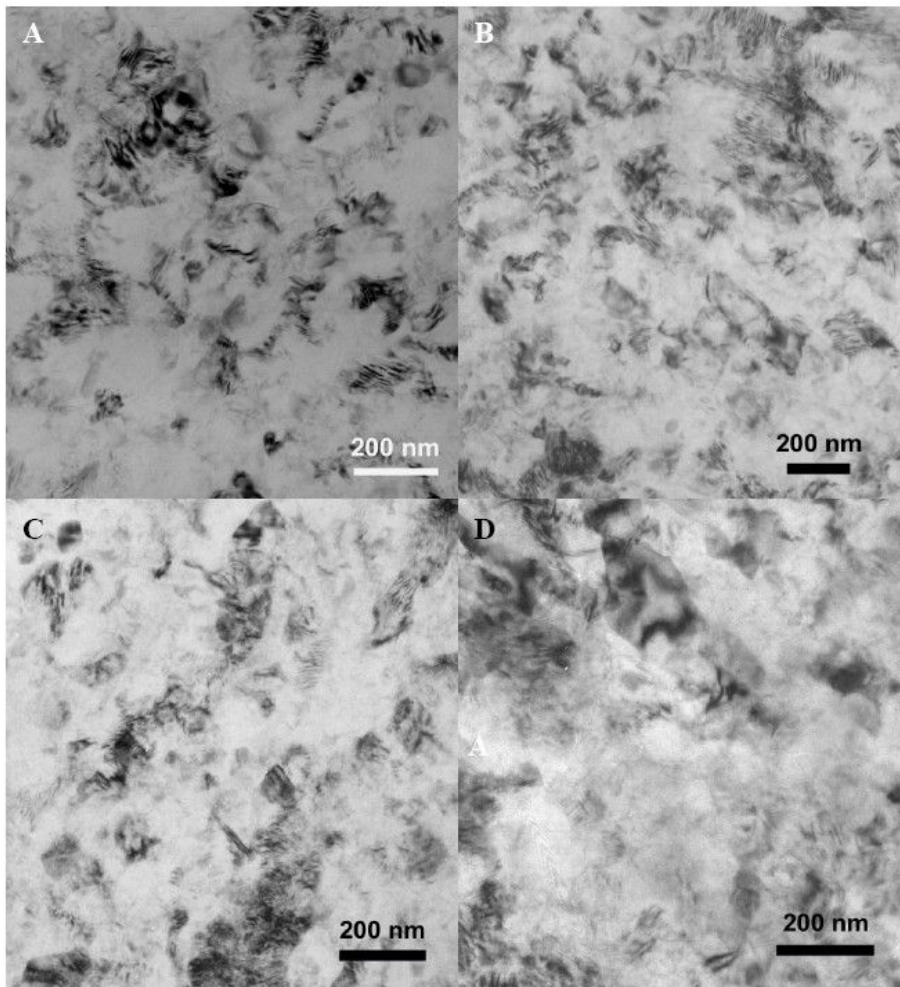


Fig. 4 Bright-field TEM images of UFG Mg₃Tb₂Nd: (A) as-deformed specimen, (B) annealed up to 80°C , (C) annealed up to 140°C , and (D) annealed up to 180°C .

Microstructure development of HPT-deformed Mg₃Tb₂Nd includes not only the precipitation effects, but also the recovery of the defects introduced by SPD. The intensity I_2 of positrons trapped at dislocations exhibits an abrupt decrease in the temperature range $(100-180)^\circ\text{C}$, see Fig. 2B. It gives a clear evidence for a recovery of dislocations occurring in this temperature interval. A single component PL spectrum above 180°C indicates that dislocation density dropped below $\approx 10^{12}\text{m}^{-2}$. Recovery of dislocations can be seen also on TEM micrographs shown in Fig. 4. Although dislocation density decreases, no grain growth was detected by TEM up to 200°C , see Fig. 4. Thus, UFG Mg₃Tb₂Nd alloy exhibits relatively high thermal stability of UFG structure which is favorable

for further applications. Precipitation of β'' phase occurs at similar temperatures as in the coarse grained alloy and causes a remarkable hardening, see Fig. 2D. As it has been already explained, PL spectroscopy is insensitive to the precipitation of coherent β'' phase. One can see in Fig. 2B that the intensity I_2 starts to increase again in the sample annealed up to 220°C and exhibits maximum at 260°C. The recovery of dislocations was completed already at 180°C. Hence, this increase of I_2 is not connected with dislocations, but occurs due to positron trapping at defects introduced by precipitation of the β_1 phase particles. The lifetime of the defect component which appeared above 220°C lays again around 256 ps. This component comes from positrons trapped at the misfit defects at incoherent interfaces of the β_1 phase observed by TEM after annealing up to 240°C in the form of fine prismatic plates. Precipitation of the β_1 phase is reflected also by an increase of microhardness. After annealing above 260°C, the behavior of I_2 is reversed and it gradually decreases in similar manner as in the coarse grained alloy. The difference between HPT-deformed and coarse grained alloy consists in the fact that precipitation of β_1 phase starts in UFG alloy already at 220°C. As a consequence, the maximum of I_2 and the peak hardness in the HPT-deformed alloy are shifted to about of 80°C lower temperatures compared to the coarse grained alloy. Thus, precipitation of β_1 phase and likely also shape transformation of β'' phase start at significantly lower temperatures in HPT-deformed alloy. It has two reasons: (i) Extremely small grain size leads to a significant volume fraction of grain boundaries. Defects at grain boundaries serve as nucleation centers for the second phase particles. (ii) Diffusivity of Tb and Nd atoms is enhanced by a possibility to diffuse along grain boundaries. Both these factors facilitate precipitation effects in the UFG alloy and shift precipitation of β_1 phase to lower temperatures.

Summary

HPT-deformed Mg₃Tb₂Nd alloy exhibits a grain size around 100 nm and a high density of homogeneously distributed dislocations. The UFG structure leads to a significant rise of hardness of the HPT-deformed alloy. Temperature development of microstructure of the HPT-deformed alloy was studied and compared with the coarse grained sample. Full recovery of dislocations in the HPT-deformed alloy takes place in relatively narrow temperature interval (100-180)°C. The precipitation sequence in the alloy with UFG structure differs from that in the coarse grained alloy. Namely the precipitation of the β_1 phase starts at remarkably lower temperatures.

References

- [1] B.L. Mordike, Mat. Sci. Eng. A Vol. 324 (2002), p. 103.
- [2] V. Neubert, I. Stulikova, B. Smola, B.L. Mordike, M. Vlach, A. Bakkar, J. Pelcova, Mater. Sci. Eng. A, Vol. 462 (2007), p. 358.
- [3] R.Z. Valiev, R.K. Islamgaliev, I.V., Alexandrov, Prog. Mat. Sci. 45 (2000), p. 103.
- [4] P. Hautojärvi, C. Corbel, in: *Proceedings of the International School of Physics "Enrico Fermi"*, edited by A. Dupasquier, A.P. Mills, Course CXXV, IOS Press, Varena (1995), p. 491.
- [5] I. Stulikova, B. Smola, N. Zaludova, M. Vlach, J. Pelcova, Kov. Mater. Vol. 43 (2005), p. 272.
- [6] F. Becvar, J. Cizek, L. Lestak, I. Novotny, I. Prochazka, F. Sebesta, Nucl. Instr. Meth. A Vol. 443 (2000), p. 557.
- [7] J. Cizek, I. Prochazka, F. Becvar, I. Stulikova, B. Smola, R. Kuzel, V. Cherkaska, R.K. Islamgaliev, O. Kulyasova, phys. stat. sol. (a) Vol. 203 (2006), p. 466.
- [8] J. Cizek, I. Prochazka, I. Stulikova, B. Smola, R. Kuzel, V. Cherkaska, R.K. Islamgaliev, O. Kulyasova, in: *Magnesium 2003*, edited by K.U. Kainer, Wiley-VCH Weinheim (2003), p. 202.